

USE OF MISFIT STRAIN TO REMOVE DISLOCATIONS FROM EPITAXIAL THIN FILMS

J. W. MATTHEWS, A. E. BLAKESLEE AND S. MADER*

IBM Thomas J. Watson Research Center, Yorktown Heights, N.Y. 10598 (U.S.A.)

(Received September 16, 1975; accepted October 9, 1975)

Misfit strain can be used to drive threading dislocations out of epitaxial films and thus to improve their perfection. This process is influenced by film thickness, the orientation of the interface, the dimensions of the interface parallel to its plane, and the misfit between film and substrate. A simple theoretical model, and experimental observations made on deposits of Ga(As, P) on GaAs, suggest that it is desirable for the film thickness to be small. This in turn implies that the misfit should be large. It should not, however, be large enough to cause dislocation nucleation. If the film is face-centered cubic, and the threading dislocations are uniformly distributed over the $\langle 110 \rangle$ {111} slip systems, then the most desirable interface orientations lie near {012} or {013}. If the Burgers vectors of the threading dislocations are not uniformly distributed then other interfaces may become desirable. Multilayers are able to remove threading dislocations more effectively than single films.

1. INTRODUCTION

Misfit strain can be used to drive threading dislocations to the edge of epitaxial thin films and thus to improve film perfection¹⁻⁵. The aims of this paper are to discuss some of the factors that influence this improvement and to present experimental results obtained on Ga(As, P)-GaAs specimens. These results provide experimental support for part of the discussion that precedes them.

We begin by considering the film thickness at which threading dislocations glide to the edge of the sample and escape, the density of threading dislocations that can be removed by glide, the influence of interface orientation on dislocation removal, the multiplication of threading dislocations, and the generation of new threading dislocations by the nucleation of half-loops.

* Present address: IBM Systems Products Division, East Fishkill Facility, Hopewell Junction, N.Y. 12533, U.S.A.

2. CONDITIONS FOR THE REMOVAL OF THREADING DISLOCATIONS

2.1. Critical thickness for the removal of threading dislocations

The removal of a threading dislocation as a result of the force exerted on it by the misfit strain is illustrated in Fig. 1. A in this figure is a threading dislocation that extends from the substrate to the free surface of the epitaxial film.

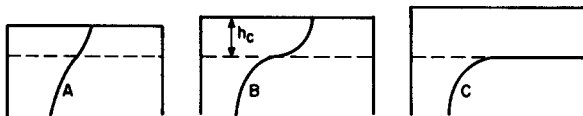


Fig. 1. Stages in the removal of a threading dislocation from an epitaxial thin film.

This dislocation bows under the influence of the misfit strain⁶ and, when the film thickness exceeds a critical value⁷, it moves to the edge of the sample and escapes. Bowing and motion to the specimen edge are shown by B and C.

The thickness at which the dislocation moves to the edge of the specimen is approximately

$$h_c = \frac{b(1 - v \cos^2 \alpha)}{8\pi f(1 + v) \cos \lambda} \ln \left(\frac{h_c}{b} \right) \quad (1)$$

where b is the strength of the threading dislocation, v is Poisson's ratio, f is the misfit between the stress-free lattice parameters of film and substrate, α is the angle between the Burgers vector \mathbf{b} and the length of dislocation line that lies in the interface plane and λ is the angle between \mathbf{b} and that direction in the interface that is perpendicular to the line of intersection of the slip plane and the interface.

For a sample with $b = 4 \text{ \AA}$, $v = 0.33$, $f = 0.01$ and $\cos \lambda = \cos \alpha = \frac{1}{2}$ the critical thickness h_c is 60 \AA .

2.2. The number of dislocations that can be removed by glide

The number of threading dislocations that can be removed by misfit strain depends to a small extent on the orientation of the interface and on the interface shape. In the simple and approximate calculation made below these dependences are neglected. We consider the removal of threading dislocations from bicrystals with a particular geometry. This geometry is similar to that of the specimens described in Sections 3 and 4. We assume that the interface is (001) and that it is a square of side L . The edges of the square are assumed to be parallel to the $\langle 110 \rangle$ directions in (001). The Burgers vectors of the threading dislocations are assumed to be of type $\frac{1}{2}a \langle 110 \rangle$ and to be inclined at 45° to (001). These threading dislocations move by glide on $\{111\}$ planes and, when they do so, they generate misfit dislocations with lines parallel to the $\langle 110 \rangle$ directions in (001).

If all threading dislocations glide to the specimen edge then the average length of misfit dislocation lines is $L/2$. If the number of threading dislocations

per unit area is ρ then the length of misfit dislocation line per unit area is

$$\rho L/2 \quad (2)$$

As half of the misfit dislocations lie along one $\langle 110 \rangle$ direction in the interface and half lie along the other, the average separation of parallel misfit dislocations is

$$4/\rho L \quad (3)$$

If the misfit accommodated by dislocations is δ then the average separation of parallel misfit dislocations is also equal to

$$(b \cos \lambda)/\delta \quad (4)$$

$\cos \lambda = \frac{1}{2}$ for specimens with the geometry considered above. Thus the density of threading dislocations removed by glide is

$$\rho = 8\delta/bL \quad (5)$$

The upper limit to the density of threading dislocations that can be removed is obtained by setting δ equal to the misfit f . This upper limit is therefore

$$\rho_{\max} = 8f/bL \quad (6)$$

This value will not be approached unless there are no serious impediments to the migration of threading dislocations¹ and the film thickness is⁸ well above h_c . For a sample with $b = 4 \text{ \AA}$, $L = 1 \text{ cm}$ and $f = 0.01$, $\rho_{\max} = 2 \times 10^6 \text{ cm}^{-2}$.

2.3. Effect of interface orientation

The effect of interface orientation on the removal of threading dislocations by glide has been discussed by Mader and Matthews². They point out that removal of all threading dislocations requires that every threading dislocation experience a glide force. This condition can be stated in a different but equivalent way. The alternative statement is that h_c must be finite for every threading dislocation. This means (see eqn. (1)) that $\cos \lambda$ must not be zero for any threading dislocation. For this to be true there must be no slip planes perpendicular to the film plane. Also, there must be no slip directions parallel to the film plane. These conditions for cubic crystals with $\langle 110 \rangle \{111\}$ slip systems are summarized in Fig. 2. This figure has been constructed on the assumption that the threading dislocations are evenly distributed over all the $\langle 110 \rangle$ slip directions and $\{111\}$ slip planes. The heavy broken line shows the interface orientations that must be avoided if there are to be no slip planes perpendicular to the film plane. The heavy full lines give the orientations that must be avoided if there are to be no slip directions parallel to the film plane. Desirable interface orientations lie inside the dotted region. Two low index interfaces within this region are (012) and (013).

Experimental evidence that GaAs crystals grown by the horizontal Bridgman technique are dislocation-free when the growth axis is parallel to $\langle 013 \rangle$ has been obtained⁹. If the seed crystals used in these experiments had lattice para-

meters that differed slightly from those of the crystals grown on them, then the perfection of the $<013>$ crystals may have been a consequence of the orientation effects discussed above.

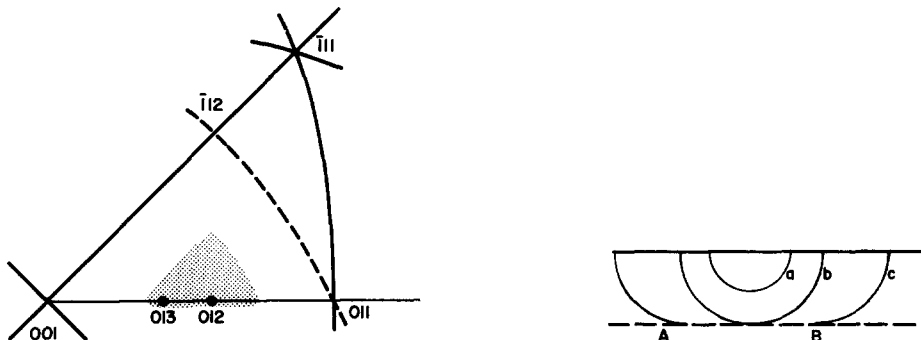


Fig. 2. Unit stereographic triangle summarizing the influence of interface orientation on the removal of threading dislocations by glide. Undesirable interface orientations are shown by heavy full and heavy broken lines. Desirable orientations lie inside the dotted region.

Fig. 3. Stages in the nucleation and growth of a dislocation half-loop.

If the threading dislocations are not evenly distributed over the possible slip systems, then interfaces outside the dotted area in Fig. 2 may become desirable. (001) interfaces are desirable if all the threading dislocations present have Burgers vectors along the $<110>$ directions inclined at 45° to (001). The (001) specimens described in Section 4 were suitable for dislocation removal because the Burgers vectors of almost all threading dislocations were inclined at 45° to (001).

2.4. Misfit needed for nucleation of dislocation half-loops

If the relief of misfit strain is to be accompanied by a net reduction in the density of threading dislocations, then processes that increase dislocation density should be curbed. One process that can lead to an increase in density is the nucleation of half-loops^{1, 8, 10} illustrated in Fig. 3. If we assume that the thickness of the film in Fig. 3 exceeds h_c by an infinitesimal amount then curve a is a sub-critical loop, curve b is critical and curve c is stable under the misfit strain.

Nucleation of dislocation loops and half-loops has been discussed by Frank¹¹ and Hirth¹². If the crystal surface (before nucleation) is perfectly flat and the dislocations nucleated at this surface are complete then the energies that need to be considered are the energy of the half-loop, the elastic energy released by the loop, and the energy of the surface created by the loop. If the loop is imperfect then the energy of the stacking fault associated with the loop should also be included. However, the energy of the stacking fault is negligible unless the stacking fault energy of the film material is unusually high ($\gtrsim 200 \text{ erg cm}^{-2}$).

If the crystal surface is not perfectly flat before nucleation then, as Hirth¹² has pointed out, the formation of a half-loop can remove or reduce the area

of a surface step. As the surfaces of our vapor-grown samples were not perfectly flat and step removal aids nucleation, we shall assume that the area of exposed surface is reduced by the nucleation of half-loops.

The energy of a semicircular shear loop of radius R is approximately¹³

$$\frac{Gb^2R}{8} \frac{2-v}{1-v} \ln \left(\frac{8R}{e^2b} \right) \quad (7)$$

where G is the shear modulus. The elastic energy released by the loop is

$$\pi R^2 \frac{G(1+v)}{1-v} fb \cos \lambda \cos \phi \quad (8)$$

where ϕ is the angle between the film surface and the normal to the slip plane. The energy of the surface removed by the half-loop is

$$2R\sigma b \sin \alpha \quad (9)$$

where σ is the surface energy of the film material: if we assume that $\sigma = Gb/8$ then the energy of the half-loop is

$$E = \frac{GbR}{8(1-v)} \left\{ b(2-v) \ln \left(\frac{8R}{e^2b} \right) - 8\pi R f(1+v) \cos \lambda \cos \phi - 2b(1-v) \sin \alpha \right\} \quad (10)$$

E is zero at $R = 0$, rises to a maximum value, the activation energy, and then decreases. The radius at which E is a maximum is

$$R_c = \frac{b(2-v) \{ \ln (8R/e^2b) + 1 \} - 2b(1-v) \sin \alpha}{16\pi f(1+v) \cos \lambda \cos \phi} \quad (11)$$

Equations (10) and (11) and suitable values for the constants ($G = 2.5 \times 10^{11}$ dyn cm⁻², $b = 4$ Å, $v = 0.33$, $\sin \alpha = (3)^{1/2}/2$, $\cos \lambda = \frac{1}{2}$, $\cos \phi = \frac{2}{3}$) have been used to find the activation energy for nucleation as a function of f . From this information the following conclusions can be drawn. If the activation energy available to form a dislocation is $50kT$ then the misfit needed for nucleation in GaAs or Ga(As, P) alloys, at 750 °C, is almost 0.02. If we follow Hirth¹² and assume that the energy available is $88kT$ then the misfit needed is 0.017.

If there are high surface steps, precipitate particles, cracks or other defects that cause the local stress to rise above the average value then dislocation nucleation may occur at lower values of misfit than suggested above. Dislocation loops or half-loops formed in regions of high local stress may grow further under misfit stress to generate misfit dislocation lines¹ as shown in Fig. 3. The film thickness at which they will generate misfit dislocations is approximately the same as that required for the operation of the process illustrated in Fig. 1.

One rather interesting prediction of the nucleation calculations concerns the nature of the half-loops. If eqns. (10) and (11) are modified to include the energy of a stacking fault inside the half-loop and the stacking fault energy of

Ga(As, P) is substituted¹⁴, it is found that the misfit needed to nucleate an imperfect glide loop is smaller than that needed for a perfect one^{12, 15}. Observations made on the dislocations present in GaAs or Ga(As, P) specimens, however, have not revealed imperfect loops. All loops detected so far¹⁶ have been complete and have had Burgers vectors of type $\frac{1}{2}a <110>$ inclined at 45° to (001). The reason for this discrepancy between predictions and experiment is not known. It is possible that the formation of complete dislocations takes place in two steps. First, an imperfect half-loop and stacking fault are made. Later, a second imperfect loop is made inside the first. This second loop removes the fault and converts the first partial into a complete dislocation. Processes of this type have been observed in metallic thin films by Cherns¹⁷. However, nucleation calculations similar to the one performed above suggest that the creation of a second partial (with a suitable Burgers vector) is improbable in our samples.

Before we leave nucleation it is worth emphasizing that the equation used for the energy of a half-loop does not include the energy of the dislocation core. If this energy were included then the estimates of the misfit needed for nucleation would be somewhat larger than those given above. A discussion of the effects of core energy on dislocation nucleation is given by Brown *et al.*¹⁸

2.5. Multiplication of threading dislocations

The relaxation of misfit strain by the processes illustrated in Figs. 1 and 3 is an example of plastic deformation. Studies of the plastic deformation of macroscopic crystals indicate that deformation is invariably accompanied by an increase in the density of dislocation lines¹⁹. This leads one to expect the relaxation of misfit strain in thin films to be accompanied by an increase in the number of threading dislocations. In this section we examine the conditions that might be expected to lead to dislocation multiplication in films and determine the conditions under which multiplication can be curbed. The assumptions on which the discussion is based are as follows.

- (1) An isolated dislocation moving in a perfect crystal cannot multiply.
- (2) Multiplication of threading dislocations requires interaction between at least two threading dislocations.

If these postulates are valid, then the conditions which prevent multiplication are those that avoid interaction. The mean free path of a threading dislocation is^{20, 21}

$$l = 1/r\rho \quad (12)$$

where r is the distance over which dislocations interact. In (001) films of f.c.c. crystals, the four {111} slip planes are all inclined at 54°44' to the film plane. In these samples r is^{20, 21} of order h . If we assume that $r = h$ then

$$l = 1/h\rho \quad (13)$$

To illustrate the predictions of this expression consider two square samples with $L = 1$ cm and $\rho = 10^4 \text{ cm}^{-2}$. Suppose that the thicknesses of the epitaxial layers are 10 μm in the first sample and 100 Å in the second. The values of l for these specimens are 0.1 cm and 100 cm, respectively. Thus, interaction between

dislocations would be common in the first sample and rare in the second. This means that dislocation multiplication would be probable in the thick film and that dislocation escape would be probable in the thin one. Experimental results consistent with these predictions are described in Sections 3 and 4.

Small values of h imply large values of f . Removal of threading dislocations from a Ga(As, P) film 100 Å thick requires a misfit (see eqn. (1)) of at least 0.007.

3. OBSERVATIONS ON THICK FILMS

3.1. *Experimental details*

Epitaxial deposits of $\text{GaAs}_{1-x}\text{P}_x$ on GaAs substrates are convenient for studying the effect of misfit strain on threading dislocations. This is partly because the magnitude of the misfit can be changed by changing the value of x and partly because accurate values for the density of threading dislocations can be obtained.

The Ga(As, P) films described here were made by chemical vapor deposition using the $\text{Ga-AsH}_3-\text{PH}_3-\text{HCl-H}_2$ vapor system²². In this system GaCl is formed by reaction of Ga with HCl and transported by the H_2 carrier gas, with AsH_3 and PH_3 , into the deposition zone. Reactive deposition produces an epitaxial layer of $\text{GaAs}_{1-x}\text{P}_x$ on the substrate surface. The value of x is controlled by the quantity of PH_3 added to the carrier gas. The deposit thickness is controlled by the duration of the deposition process. The samples described in this section were all about 10 µm thick.

The surfaces of the GaAs substrates were chemically polished and were inclined at between 2° and 3° to (001). The rotation away from (001) was about a <110> axis in (001). The substrate temperature during film growth was 750 °C.

The density of threading dislocations in the substrates and in the epitaxial deposits was determined using etch pits. The etchant used for the substrates was the KOH solution described by Grabmaier and Watson²³. Etch pits on the surfaces of the epitaxial layers were made by immersing the samples for 5 to 10 min in an AB etch²⁴ at room temperature.

To observe dislocations in the interface between overgrowth and substrate, samples were angle-polished to expose a (111) plane. Etch pits were produced on this plane by a modified Richards-Crocker (RC-1) etch²⁵.

3.2. *Results*

Four bicrystals were prepared and examined. The results are summarized

TABLE I

A COMPARISON OF THE DENSITY ρ_s OF THREADING DISLOCATIONS IN THE SUBSTRATE WITH THE DENSITY ρ_d IN THE EPITAXIAL DEPOSIT

Specimen	x	f	$\rho_s (\text{cm}^{-2})$	$\rho_d (\text{cm}^{-2})$
1	0	0	3.4×10^3	5.7×10^3
2	0	0	7.2×10^2	1.3×10^3
3	1.2×10^{-2}	4.3×10^{-4}	1.3×10^3	4.7×10^4
4	1.4×10^{-2}	5.0×10^{-4}	2.5×10^2	1.0×10^4

in Table I. In specimens 1 and 2 the phosphorus concentration was zero. These specimens were made in order to determine whether there was a significant change in the density of threading dislocations when the misfit strain was zero. Comparison of ρ_s and ρ_d for these samples shows that in both cases there was a small increase in dislocation density during film growth. The reasons for the increase are not known. However, the important result is that the increase was small.

In specimens 3 and 4 the values of f were 4.3×10^{-4} and 5×10^{-4} , respectively. Comparison of ρ_s and ρ_d for these samples shows that the density of threading dislocations increased about forty-fold during film growth. This result is consistent with predictions made for thick films in Section 2.5.

Evidence that the increase in dislocation density shown by specimens 3 and 4 was associated with dislocation glide is provided by optical micrographs like the one in Fig. 4. This figure shows the surface of an etched Ga(As, P) layer. The arrowed pale and dark dots and streaks are etch pits at threading dislocations. The origin of the large dots such as the one at X is not known. The indistinct dark and light lines parallel to $\langle 110 \rangle$ directions are minute elevations and depressions in the sample surface. These elevations and depressions are characteristic of (001) specimens that have deformed by glide on $\{111\}$ planes²⁶.

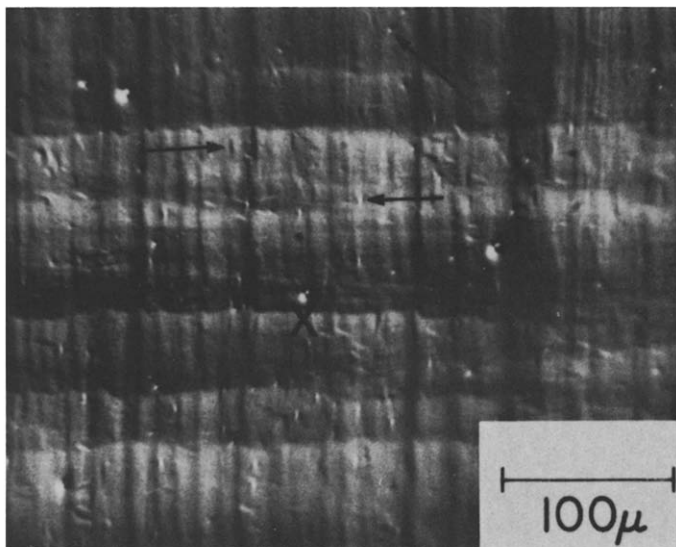


Fig. 4. Optical micrograph of the surface of a thick, etched epitaxial layer of Ga(As,P) on GaAs. The borders of the figure are parallel to $\langle 110 \rangle$.

Although the plastic deformation that accompanied the growth of specimens 3 and 4 was accompanied by a net increase in the density of threading dislocations, there is evidence that some dislocations were removed by the mechanism described in Section 2.1. This evidence was provided by pits formed where the interface met (111) surfaces that were polished and etched as described in Section 3.1.

The number of pits per centimeter of interface was 1.8×10^3 in specimen 3 and 5.2×10^3 in specimen 4. If we assume that the dislocations responsible for the pits had Burgers vectors of type $\frac{1}{2}a <110>$ inclined at 45° to (001), then the misfit accommodated by them was 3.6×10^{-5} in specimen 3 and 1.04×10^{-4} in specimen 4. These values are smaller than predicted by van der Merwe²⁷ and Matthews⁸. This suggests that motion of threading dislocations to the edges of the samples was impeded in some way. One explanation for this impediment is as follows. Threading dislocations interacted with one another during glide, and this interaction led not only to an increase in the density of threading dislocations but also to some work hardening of the deposit^{19, 21}. An alternative explanation is that motion to the specimen edge was hindered by the Peierls stress¹.

4. OBSERVATIONS ON MULTILAYERS COMPOSED OF THIN FILMS

4.1. *Experimental details*

Specimens suitable for testing the effect of film thickness on dislocation removal and for measuring the misfit at which dislocation nucleation takes place were prepared²⁸ for the semiconducting superlattice device proposed by Esaki and Tsu²⁹. Specimens were made in two forms. The first form consisted of many (60–120) thin (70–700 Å) alternating layers of GaAs and $\text{GaAs}_{0.5}\text{P}_{0.5}$ grown epitaxially on GaAs substrates¹⁶. The second form resembled the first in that it contained a multilayer composed of many alternating GaAs and $\text{GaAs}_{0.5}\text{P}_{0.5}$ layers; it differed in that the growth of the multilayer was preceded by the deposition of a graded layer on the GaAs wafer⁵. The composition of this graded layer changed from pure GaAs at the substrate surface to $\text{GaAs}_{0.77}\text{P}_{0.23}$ at the surface on which the multilayer was grown. This final composition was chosen so that the lattice parameter of the upper surface of the graded layer matched the lattice parameter of the multilayer taken as a whole³⁰.

The matching of substrate to multilayer was done in order to prevent the generation of dislocations to accommodate misfit between multilayer and substrate. The importance of matching was suggested by studies of the dislocations present in multilayers grown on unmatched substrates¹⁶. The effect of matching⁵ was to reduce the density of threading dislocations by a factor of at least 10^4 . Multilayers grown on unmatched substrates contained about 10^8 threading dislocations per square centimeter. Those grown on matched substrates contained less than 10^4 cm^{-2} .

All multilayers were grown by chemical vapor deposition using apparatus described elsewhere²⁸. An important feature of this apparatus was its ability to inject PH_3 into an AsH_3 vapor stream so that there was little mixing of the AsH_3 and $\text{PH}_3 + \text{AsH}_3$ pulses on their way to the deposition zone. This ensured that the composition changes from one layer to the next were rapid. However, as some mixing of the pulses is inevitable the composition changes were not perfectly abrupt. The duration of the PH_3 pulse was controlled by an electronic timer. The relative thicknesses of the GaAs and $\text{Ga}(\text{As}, \text{P})$ layers could be adjusted by varying the ratio of the off to on times. However, the on and off times were equal in all the specimens described here. This ensured that the thicknesses of the GaAs and

Ga(As, P) layers were very nearly equal. Layer thicknesses were determined from scanning electron micrographs of the multilayers viewed from the side or from the positions of satellite peaks in X-ray diffraction patterns³¹.

The dislocations present in the samples were detected using either etch pits or transmission electron microscopy. Specimens were prepared for transmission electron microscopy in the following way¹⁶. Wafers were lapped on the substrate side to a total thickness of 150 μm and cleaved into small squares so as to fit into the sample holder of the microscope. The multilayer was then etched from the substrate side by a fine jet. The liquid in the jet was made by adding 15 drops of Br_2 to 100 ml of CH_3OH . Etching was stopped when a small hole appeared in the sample.

The etch pits used to detect interfacial and threading dislocations were made in polished (111) surfaces using the (RC-1) etch as described in Section 3.1.

4.2. *Observations*

4.2.1. *Multilayers on unmatched substrates*

Multilayers grown on unmatched substrates contained dislocations of three kinds.

- (1) The first kind are dislocations that accommodate misfit between individual layers.
- (2) Then we have dislocations that accommodate misfit between the multilayer taken as a whole and its substrate.
- (3) Finally we have threading dislocations.

These dislocations have been described elsewhere and the descriptions of them will not be duplicated here¹⁶. The important features of the dislocations so far as this paper is concerned are as follows.

(a) The dislocations present to accommodate misfit between layers were often in the form of elongated loops. The formation of these loops is thought to begin with the nucleation of half-loops as discussed in Section 2.4 (see Fig. 9 of ref. 16).

(b) The density of threading dislocations was less than $5 \times 10^4 \text{ cm}^{-2}$ in the substrates but 10^8 cm^{-2} in the multilayers. This increase is thought to arise partly from the nucleation of half-loops in the first epitaxial film in the multilayer (see Fig. 8 of ref. 16) and partly from multiplication processes in the multilayer³⁰.

If (a) and (b) are correct then the 1.8% misfit between GaAs and the $\text{Ga}(\text{As}_{0.5}\text{P}_{0.5})$ is large enough to cause the nucleation of half-loops at 750 °C. This result is consistent with the calculation in Section 2.4.

4.2.2. *Multilayers on matched substrates*

These multilayers differed from the unmatched ones in that they did not contain any dislocation loops to accomodate misfit between layers. Also, they contained so few threading dislocations that we have not detected any by transmission electron microscopy⁵. This means that the density of threading dislocations was less than 10^4 cm^{-2} . This result has been confirmed by optical images of etch pits.

The absence of threading and misfit dislocations from matched multilayers suggests that the approximately 0.9% misfit between $\text{GaAs}_{0.77}\text{P}_{0.23}$ and GaAs

or $\text{GaAs}_{0.5}\text{P}_{0.5}$ is insufficient to nucleate dislocation half-loops. This result is consistent with the calculation in Section 2.4.

Before we proceed with discussion of the elimination of threading dislocations from matched multilayers it is worth emphasizing that the results described so far in this section were not obtained from the first few layers of the multilayer. The method of sample preparation described in Section 4.1 removed the early layers from all samples examined by transmission electron microscopy. This means that we do not have direct evidence for the absence of nucleation in the early layers grown on matched substrates. Also we have not made direct observations of the process illustrated in Fig. 1. Direct observations of it have been made, however, by Rozgonyi *et al.*³, Olsen *et al.*⁴ and Matthews and Jesser¹⁰.

Evidence that threading dislocations were removed in large numbers from matched multilayers has come from transmission electron microscopy⁵, from scanning electron microscopy and from optical micrographs of etched (111) polished sections. The results obtained from optical micrographs will be discussed with the aid of Fig. 5. This figure shows a section through one of the multilayers examined. A is the substrate; it consists of a GaAs wafer on which a 9 μm epitaxial film of GaAs was grown. B is the graded layer, C is a layer of constant composition ($\text{GaAs}_{0.77}\text{P}_{0.23}$), D is the multilayer and E is a layer of constant composition similar to C. The number of layers in the multilayers was 80 (*i.e.* 40 GaAs and 40 $\text{GaAs}_{0.5}\text{P}_{0.5}$). The thickness of individual layers was approximately 95 Å. The number of etch pits per square centimeter in the labelled regions was less than 10^4 in A, approximately 10^8 in B, 2×10^6 in C, less than 10^4 in D and 2×10^5 in E.



Fig. 5. A section through a "matched" multilayer. The lettered regions are discussed in the text. The numbers are the layer thicknesses in micrometers.

Fig. 6. A scanning electron micrograph of a matched multilayer viewed from the side. The dark and light lines are individual layers. C is a Ga (As, P) layer whose lattice parameter matches that of the multilayer taken as a whole. The etch pits between C and the multilayer show that there were many dislocations in the substrate-multilayer interface.

The dramatic increase in dislocation density from A to B is a well-known phenomenon described by Abrahams *et al.*³² Most of the increase is due to the misfit dislocations formed in order to accommodate the gradient in lattice parameter in B. The remainder arises from an increase in the number of threading dislocations³². This increase is thought to take place by multiplication processes

that involve interaction between dislocations as discussed in Section 2.5.

An important feature of threading dislocations in regions like B is that their Burgers vectors are not uniformly distributed over the $\langle 110 \rangle$ directions. The majority of dislocations have $\frac{1}{2}a\langle 110 \rangle$ Burgers' vectors inclined at 45° to the (almost) (001) film plane³⁴. This has an important consequence alluded to at the end of Section 2.5. The consequence is that the misfit stresses in the multilayer exert a glide force on almost all threading dislocations present. Thus one might expect almost all threading dislocations to be removed from samples like the one in Fig. 5.

The drop in dislocation density from 10^8 cm^{-2} in B to 2×10^6 in C arises largely because there is no lattice parameter gradient in C and thus no need for misfit dislocations. 2×10^6 is a measure of the density of threading dislocations in C.

The change in dislocation density from C to D is believed to result from the removal process shown in Fig. 1. Direct evidence that dislocations are present in the interface between multilayers and matched substrates is provided by scanning electron micrographs of sections through the multilayer. One of these micrographs is seen in Fig. 6. The parallel dark and light lines in this figure are images of individual layers in the multilayers and C is the layer of constant composition. The etch pits labelled y are due to dislocations in the interface between multilayer and substrate.

The reason for the increase in density from D to E in Fig. 5 is not certain. It is probable, however, that the lattice of E was not perfectly matched to D. If this was so and the number of threading dislocations in the initially deposited portion of E was not close to unity, then E would be expected to behave like specimens 3 and 4 of Section 4.1. The behavior of specimens 3 and 4 shows that a matching error of only 5×10^{-4} is sufficient to produce a rise in dislocation density similar to that from D to E. Evidence that matching errors of at least 5×10^{-4} were present in the matched multilayers has been obtained⁵.

The misfit between C and the first (GaAs) layer in the multilayer was 0.009. The calculation in Section 2.2 shows that this is barely sufficient to remove 10^6 dislocations per square centimeter. There is evidence, however, that not all dislocations were removed at the first interface. The evidence for this has come from scanning electron micrographs of multilayers viewed from the side. An etch pit due to a dislocation that seems to be in an interface other than the first is labelled x in Fig. 6.

The fact that several interfaces seem to be involved in the removal of dislocations from matched multilayers suggests that multilayers are more effective at removing threading dislocations than single layers are. That this should be so is not surprising. The upper limit to the number of threading dislocations that can be removed by a multilayer containing N layers is $N\rho_{\max}$ (see eqn. (6)).

It is possible that the effectiveness of matched multilayers is greater than this number suggests. This is because matched multilayers can remove dislocations that cannot be removed by single layers even if the density of threading dislocations in the single layers is less than ρ_{\max} . The reason for this is as follows. The elastic misfit stresses in matched multilayers change sign from one layer

to the next. Thus, if the stress in the first layer drives a threading dislocation into an obstacle, the stress in the second layer will drive the portion of the dislocation that threads the second layer away from the obstacle. This motion may take the dislocation out of the sample.

5. DISCUSSION

The results presented above indicate that misfit strain can be used to drive dislocations out of thin films. They also show that it is difficult to improve the perfection of thick films by this method. This implies that the misfit used to drive dislocations out of crystals should be large. The misfit should not, however, be so large that dislocation nucleation is probable.

One way of extending the method to thick films and small values of f is to reduce L , the dimension of the sample in the interface plane. This reduces the distance that dislocations have to travel in order to escape and so reduces the probability of interaction and multiplication. Reduction of L also has the advantage of increasing the upper limit to the density of threading dislocations that can be removed by a particular value of the misfit. That this is so is clear from eqn. (6) in Section 2.2.

Observations consistent with those described in this paper have been made by Olsen *et al.*⁴ and Abrahams *et al.*³² Abrahams *et al.* grew thick graded layers of $\text{GaAs}_{1-x}\text{P}_x$ on GaAs wafers and found that the density of threading dislocations increased. The values of thickness and misfit in these graded layers were such that the glide of threading dislocations would have been accompanied by interaction between a large fraction of them. Thus, the increase in dislocation density found by Abrahams *et al.*³² is consistent with the conditions for dislocation multiplication discussed in Section 2.5.

Most of Olsen *et al.*'s⁴ observations were made on $\text{In}_x\text{Ga}_{1-x}\text{P}$ layers grown on GaP but some experiments were performed on bicrystals of $\text{GaAs}_{1-x}\text{P}_x/\text{GaP}$, $\text{In}_x\text{Ga}_{1-x}\text{P}/\text{GaAs}$ (with $x > 0.5$) and $\text{In}_x\text{Ga}_{1-x}\text{As}/\text{GaAs}$. It was found that large abrupt changes in misfit strain were accompanied by substantial reductions in the density of threading dislocations. This result agrees with Section 2.5 and with the experimental results in Section 4.2.2.

Observations that seem at first sight to be inconsistent with the predictions of Section 2.5 and the observations of Section 3 have been made by Rozgonyi *et al.*³ They have found it possible to remove threading dislocations from specimens where the misfit was small and the film thickness large. However, their choice of film thickness was made in such a way that the probability of certain interactions between threading dislocations was small. They began by making a careful study of the behavior of threading dislocations during the growth of (Ga,Al)(As,P) films on GaAs substrates and found that, over a narrow thickness range above h_c , the threading dislocations moved by glide and cross-slip to form an array of parallel misfit dislocations. Thus, over this narrow thickness range all threading dislocations moved on slip planes that intersected the (001) film plane along only one of the two $\langle 110 \rangle$ directions in (001). This restricted motion did not lead to interactions between dislocations that resulted in obstruc-

tion either to further glide or to dislocation multiplication. The threading dislocations simply moved to the edges of the sample and escaped there. Other experiments that have revealed anisotropic glide in (001) bicrystals of III-V compounds have been performed by Abrahams *et al.*³⁵ The origin of the anisotropy is not known. The anisotropy of the Peierls stress in III-V compounds is one of several possible explanations for it.⁸

ACKNOWLEDGMENTS

We would like to thank B. Bischoff for his help with specimen preparation. The scanning electron micrograph in Fig. 6 was taken by C. G. Bremer.

REFERENCES

- 1 J. W. Matthews, S. Mader and T. B. Light, *J. Appl. Phys.*, **41** (1970) 3800.
- 2 U. S. Patent Number 3,788,890 (January, 1974), to S. Mader and J. W. Matthews.
- 3 G. A. Rozgonyi, P. M. Petroff and M. B. Panish, *J. Cryst. Growth*, **27** (1974) 106.
- 4 G. H. Olsen, M. S. Abrahams, C. J. Buiocchi and T. J. Zamerowski, *J. Appl. Phys.*, **46** (1975) 1643.
- 5 J. W. Matthews and A. E. Blakeslee, *J. Cryst. Growth*, in the press.
- 6 J. W. Matthews, *Philos. Mag.*, **13** (1966) 1207.
- 7 W. A. Jesser and J. W. Matthews, *Philos. Mag.*, **15** (1967) 1097.
- 8 J. W. Matthews, *J. Vac. Sci. Technol.*, **12** (1975) 126.
- 9 T. S. Plaskett, J. M. Woodall and A. Segmüller, *J. Electrochem. Soc.*, **118** (1971) 115.
- 10 J. W. Matthews and W. A. Jesser, *Acta Metall.*, **15** (1967) 595.
- 11 J. W. Matthews, in *Epitaxial Growth*, Academic Press, New York, 1975, p. 559.
- 12 F. C. Frank, *Symp. on Plastic Deformation of Crystalline Solids*, Carnegie Inst. of Technology, Pittsburgh, 1950, p. 89.
- 13 J. P. Hirth, in *Relation Between Structure and Strength in Metals and Alloys*, H.M.S.O., London, 1963, p. 218.
- 14 F. R. N. Nabarro, *Theory of Crystal Dislocations*, Clarendon Press, Oxford, 1967, p. 75.
- 15 S. Mader and A. E. Blakeslee, *Appl. Phys. Lett.*, **25** (1974) 365.
- 16 J. W. Matthews, *J. Appl. Phys.*, **42** (1971) 5640.
- 17 D. Cherns, *Ph. D. Dissertation*, Cambridge University, 1974.
- 18 L. M. Brown, G. R. Woolhouse and U. Valdre, *Philos. Mag.*, **17** (1968) 781.
- 19 F. R. N. Nabarro, Z. S. Basinski and D. B. Holt, *Adv. Phys.*, **13** (1964) 193.
- 20 P. Chaudhari, S. Mader and J. F. Freedman, *J. Vac. Sci. Technol.*, **6** (1969) 618.
- 21 J. W. Matthews and J. L. Crawford, *Thin Solid Films*, **5** (1970) 187.
- 22 M. G. Crawford, *Progr. Solid State Chem.*, **8** (1973) 127.
- 23 J. G. Grabmaier and C. B. Watson, *Phys. Status Solidi*, **32** (1969) K13.
- 24 M. S. Abrahams and C. J. Buiocchi, *J. Appl. Phys.*, **36** (1965) 2855.
- 25 M. S. Abrahams, *J. Appl. Phys.*, **35** (1964) 3626.
- 26 G. H. Olsen, M. S. Abrahams and T. J. Zamerowski, *J. Electrochem. Soc.*, **121** (1974) 1650.
- 27 J. H. van der Merwe, in *Single Crystal Films*, Pergamon Press, Oxford, 1964, p. 139.
- 28 A. E. Blakeslee, *J. Electrochem. Soc.*, **118** (1971) 1459.
- 29 L. Esaki and R. Tsu, *IBM J. Res. Dev.*, **14** (1970) 61.
- 30 J. W. Matthews and A. E. Blakeslee, *J. Cryst. Growth*, **29** (1975) 273.
- 31 A. Segmüller and A. E. Blakeslee, *J. Appl. Crystallogr.*, **6** (1973) 19.
- 32 M. S. Abrahams, L. R. Weisberg, C. J. Buiocchi and J. Blanc, *J. Mater. Sci.*, **4** (1969) 223.
- 33 S. Mader and A. E. Blakeslee, *IBM J. Res. Dev.*, **19** (1975) 151.
- 34 J. Washburn, G. Thomas and H. J. Queisser, *J. Appl. Phys.*, **35** (1964) 1909.
- 35 M. S. Abrahams, J. Blanc and C. J. Buiocchi, *Appl. Phys. Lett.*, **21** (1972) 185.